or $\dot{\epsilon}$ change alone. Constant structure also implies that the sample must be deforming in a macroscopically homogeneous fashion. Hence we determine V^* here in the uniform cold-drawing regime beyond the Lüders strain (which is small in AC 1220). Also implicit in our experiments is the assumption that the ratio of applied stresses pertaining to a change of strain rate or pressure is equal to the ratio of the effective *stresses* acting on the mobile species. If the applied stress τ_a is unequal to the effective stress, either because τ_a is screened by a long-range internal stress τ_i or because τ_a is amplified by a stress concentration factor K, we assume that τ_i or K does not change during P or $\dot{\epsilon}$ cycling.

Therefore, with these qualifications the experiments proceed as indicated by the test record reproduced in Fig. 1. At pressure P_1 the sample is deformed plastically to tensile stress σ_1 at which point the deformation rate is cycled by a factor of ~5, i.e., increased briefly and then decreased to the original value. On increasing $\dot{\epsilon}$ the flow stress is raised to σ_2. On decreasing $\dot{\epsilon}$ the stress reaches σ_3 from where it is then reduced to zero. The pressure is then raised to P_2, and on reloading there is an increase in flow stress from σ_3 to σ_4. The deformation rate is cycled again, then load released, and the pressure is reduced once more to P_1, and so on, until the sample fails. The parameter m is computed at each pressure from the ratio of stresses, i.e., $\ln(\dot{\epsilon}_2/\dot{\epsilon}_1)/\ln(\sigma_2/\sigma_1)$, etc. (It is not necessary to resolve to the shear component for the stress ratio.) The value of V^* computed for an increase or decrease of pressure is assigned to the mean pressure by using the geometric mean value of m (the variation of $\ln m$ with P is approximately linear) for the two pressures and the ratio of stresses, i.e., $\ln(\sigma_4/\sigma_3)$; ΔP is ~20 000 psi (1.38 kbar) except for the lowest mean pressure (0.35 kbar) where it is ≃10 000 psi. It is found that during a time period (~25 min) equal to that required to unload the sample, change pressure, and attain thermal equilibrium, aging of the specimen occurs, i.e., after unloading, the stress required to reinitiate flow on reloading (at the same pressure) is ~1–2% higher (approximately independent of pressure). Hence the apparent relative change of stress due to pressure is greater on increasing as opposed to decreasing pressure (as much as 30% at higher pressures where the relative change of σ with P is smaller). To account for this effect the values of V^* reported are the mean of successful determinations with increasing and decreasing pressure (or vice versa). Figure 1 also indicates that we determine the flow stress after a pressure (or $\dot{\epsilon}$) change by the extrapolation technique.

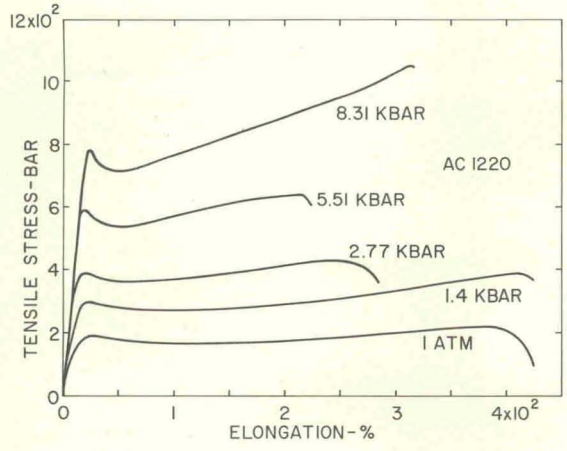

FIG. 1. Cyclic load(nominal stress)–elongation curves for AC 1220 PE indicating the change of stress with pressure and strain rate; $\dot{\epsilon}_2/\dot{\epsilon}_1 \simeq 5.9$ at 6.22 kbar and 4.8 a4 7.58 kbar.

Because we measure ratios of stresses (actually loads) it is not essential to know the true stress along the τ-ϵ curve to determine V^*. We should, however, correct for the small change of cross-sectional area which occurs when the pressure is changed. The correction amounts to $\frac{2}{3}mkT\beta$, where β is the volume compressibility. We have determined β from the results of Pastine[11] (see his Table VII) for an isotropic PE of 0.954-g/cm³ density. The calculated correction is thus slightly less than necessary for our lower-density material (0.90–0.935 g/cm³) in the isotropic state, but this is probably compensated by a reduced area compressibility of the specimen when in the cold-drawn state. It is found that an increase of m with pressure just compensates the decrease in β so that the correction term is almost constant at 8 Å³.

The experiments are conducted at room temperature (~22 °C).

RESULTS

Figure 2 shows several representative load-elongation curves for AC 1220 PE tested in water. It can be noted that the yield drop in this material is quite small. Also both the yield stress and the rate of work hardening increase with increasing pressure; the total elongation to failure decreases moderately with increasing pressure. The variation of the tensile yield stress with pressure is shown more clearly in Fig. 3; the circles correspond to specimens tested in water and the triangles correspond to those tested in pentane. The solid line shown is a quadratic least-squares fit to the water data. The yield-stress values

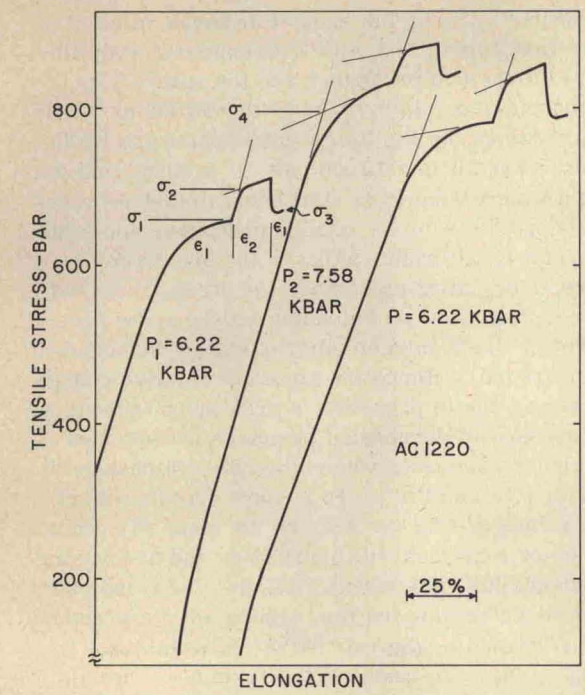

FIG. 2. Nominal stress-elongation ($\Delta L/L_0$) curves for AC 1220 PE tested at several pressures in water (stress uncorrected for the reduced area of the specimen resulting from hydrostatic compression).

in pentane fall below the solid line depending on the amount of pentane absorbed. The lowest points at a given pressure occur near saturation (> 24 h soaking in pentane).

The variation of the inverse strain-rate sensitivity of the flow stress $(\partial \ln\dot{\epsilon}/\partial \ln\sigma)_{T,P} \equiv m$, is given as a function of strain (at several pressures) and pressure (at several strains) in Figs. 4 and 5, respectively. It is evident in all cases that m decreases with increasing strain and increases strongly with increasing pressure. The slope of the curve $\ln m$ vs P in Fig. 5 is ~ 0.125 kbar^{-1}; the apparent strain dependence of this slope falls within the experimental uncertainty. According to Eq. (4) m is one of the two parameters needed to calculate V^*; the other is the partial derivative $(\partial \ln\sigma/\partial P)_{T,\dot{\epsilon}}$. This is shown in Fig. 6 for samples tested in water (circles) and pentane (triangles); the data at each pressure are obtained from 1–3 specimens. If one evaluates the derivative at each pressure from the solid curve in Fig. 3, the dashed curve in Fig. 6 is obtained. It is apparent that the data points generally fall somewhat above the yield-point curve; they also seem to follow a curve of slightly different shape. Both of these features may be accounted for to a large degree by the fact that $\partial \ln\sigma/\partial P$ increases with increasing strain at a given pressure.

We calculate V^* then by multiplying the data in Fig. 6, point by point, by the appropriate values of m and kT. Because the relative strain dependences of m and $(\partial \ln\sigma/\partial P)_{T,P}$ are nearly equal and of opposite sign, V^* is only slightly dependent on ϵ at lower pressures and apparently independent of ϵ at higher pressures. This is indicated for a few cases in Fig. 7. In an attempt to account for this small strain dependence in a final plot of V^* vs P we choose a reference strain $\epsilon = 1.25$ which

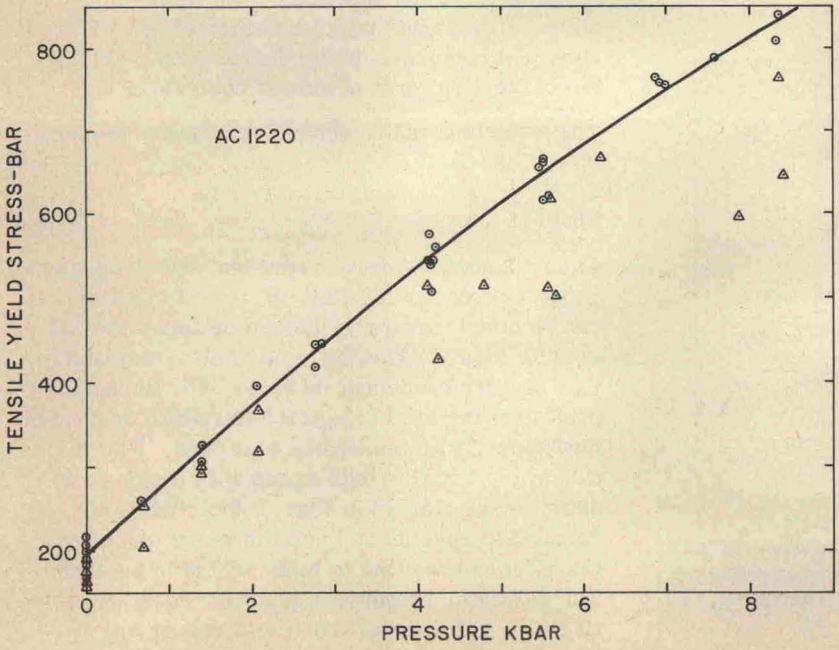

FIG. 3. Tensile yield stress (nominal) as a function of pressure for samples tested in water (circles) and pentane (triangles). The solid curve is a quadratic least-squares fit of the water data; $\sigma = 195 + 92.7P - 1.92P^2$, where σ is in bar for P in kbar. The stress is corrected for the compressibility of the samples according to the data of Pastine (Ref. 13) noted in the text.